Journal of the European Ceramic Society 21 (2001) 177–183

www.elsevier.com/locate/jeurceramsoc

Microstructural characterization and crystallization kinetics of $(1-x)TeO_2$–$xLiCl$ ($x=0.6$–0.4 mol) glasses

M.L. Öveçoğlu [a,*], G. Özen [b], B. Demirata [c], A. Genç [a]

[a] *Department of Metallurgical and Materials Engineering, Faculty of Chemical and Metallurgical Engineering, Istanbul Technical University, Maslak 80626, Istanbul, Turkey*

[b] *Department of Physics, Faculty of Science and Letters, Istanbul Technical University, Maslak 80626, Istanbul, Turkey*

[c] *Department of Chemistry, Faculty of Science and Letters, Istanbul Technical University, Maslak 80626, Istanbul, Turkey*

Received 26 February 2000; received in revised form 1 June 2000; accepted 17 June 2000

Abstract

On the basis of DTA analyses, three $(1-x)TeO_2$–$xLiCl$ ($x=0.3$, 0.35 and 0.4 mol) glasses doped with 0.005 mol of Tm_2O_3 were crystallized in the vicinity of 400°C. X-ray investigations for samples heated to 425°C (above the peak crystallization temperature) followed by quenching in air, revealed the presence of the paratellurite (TeO_2) as the only crystallizing phase in all glass compositions. SEM investigations revealed that the paratellurite crystals formed in these glasses as a result of surface crystallization were trigonal in shape, between 40 and 50 μm in length, 7 and 15 μm in width and 5 and 9 μm in depth. DTA analyses were carried out on the $0.7TeO_2$–$0.3LiCl$ glass at different heating rates and an activation energy value of 238 kJ/mol for surface crystallization was determined graphically from a Kissinger-type plot using the analysis of Matusita and Sakka (Matusita, K. and Sakka, S., Kinetic study on crystallization of glass by differential thermal analysis — criterion on application of Kissinger plot. *J. Non-cryst. Solids*. **38&39**, 741–746.).

Keywords: Crystallisation; Glasses; LiCl; TeO_2; Microstructure-final

1. Introduction

In comparison with silicate[1,2] and borate[3] glasses, tellurite glasses have more advantages as frequency upconversion laser hosts due to their physical properties such as low melting temperature, high dielectric constant,[4,5] high refractive index,[4] large third order nonlinear susceptibility[5,6] and better infrared transmissivity.[7] Furthermore, they present large transparency between the near ultraviolet to the middle infrared region. In addition, they are resistant to atmospheric moisture and capable of incorporating large concentrations of rare earth ions such as Tm^{3+} into the matrix.[8]

Currently there exists a substantial amount of literature which reported the thermal, optical and physical properties of TeO_2 based glasses[9–24] and regarding the structure of pure TeO_2 and M_2O–TeO_2 (where M = Li, Na, K, Rb and Cs) glasses[19–24] characterized by using X-ray diffraction,[19–21] neutron diffraction, NMR,[23] ZAFS[21] and Mösbauer spectroscopy techniques.[21,22] However, no reported literature is available on the formation of crystalline phases in TeO_2–LiCl glass systems and thus no detailed studies related to the crystallization kinetics have been conducted. The present study aims to fulfill this task.

The present paper focuses on the microstructural characterization and the crystallization kinetics of the crystallizing phase in the $(1-x)TeO_2$–$xLiCl$ ($x=0.6$–0.7 mol) binary system. Three different glass compositions, viz. the $0.6TeO_2$–0.4LiCl, $0.65TeO_2$–0.35LiCl and the $0.7TeO_2$–0.3LiCl glass doped with 0.005 mol of Tm_2O_3, were investigated using DTA, X-ray diffractometry and SEM techniques. Further, DTA analyses at different heating rates were used to determine the activation energy for surface crystallization.

2. Experimental procedure

2.1. Glass synthesis

Three tellurite glasses were prepared to constitute the compositions of 60 mol% TeO_2–40 mol% LiCl, 65 mol% TeO_2–35 mol% LiCl and 70 mol% TeO_2–30 mol% LiCl doped with 0.5 mol% Tm_2O_3 (now hereafter referred to as the $0.6TeO_2$–0.4LiCl, $0.65TeO_2$–0.35LiCl and $0.7TeO_2$–0.3LiCl glasses, respectively). Reagent grade TeO_2 (99.999% purity, Aldrich Chemical Company), LiCl

* Corresponding author.
E-mail adress: ovecoglu@itu.edu.tr (M.L. Öveçoğlu).

0955-2219/01/$ - see front matter
PII: S0955-2219(00)00187-4

(99.999% purity, Aldrich Chemical Company) and Tm_2O_3 (99.9% purity, Sigma Chemical Company) powders were used in this investigation. Batches of 7 g in size were thoroughly mixed and melted in air using a Pt-crucible with a closed lid in an electrically heated furnace at 700–750°C for 30 h. Following that, the melts were removed from the furnace at 750°C and quenched in air by casting and pressing between two rectangular graphite slabs at room temperature. A series of wet chemistry analyses were done on bulk as-quenched and heat-treated TeO_2–LiCl samples. These analyses have shown that the initial elemental stoichiometry of the bulk glass samples did not change after quenching and heat-treating. Further, a Zmax 30 Boron-up light element energy dispersive spectrometer (EDS) detector attached to JEOL™ Model JSM-T330 scanning electron microscope (SEM) was used to detect any compositional segregation in the microstructure which did not take place. Based on the wet chemistry and EDS analyses, it can be stated that the volatilization losses were negligible during melting due to using an inert Pt-crucible with a closed lid. Bahgat et al.[25] have also reported that using a Pt-crucible is the most effective procedure against high volatilization of TeO_2 at high temperatures.

2.2. Thermal behaviour

Differential thermal analysis (DTA) scans of as-cast glass specimens were carried out in a Rigaku Thermoflex thermal analyzer equipped with a PTC-10A temperature control unit in order to determine the characteristic glass transition temperatures (T_g), crystallization (T_c) and the peak crystallization temperatures (T_p). After pulverizing and grinding as-cast glass, static non-isothermal DTA experiments were performed by heating 20 mg glass powder at heating rates of 5, 10, 15 and 20°C in a Pt-crucible and using the same amount of Al_2O_3 as the reference material in the temperature range between 20 and 600°C. The crucibles used were matched pairs made of platinum and the temperature precision was ±1°C. The T_g temperature is a selected as mid-point between the onset and the minimum temperature. Whereas the T_c temperature is measured at the onset of crystallization, the T_p temperature is measured at the peak of crystallization. Crystallization experiments of annealed glass samples were carried out in a muffle furnace which had an approximate heating rate of 10°C/min.

2.3. Microstructural characterization

The microstructural characterization of the as-cast and crystallized glass samples were carried out using both electron microscopy and X-ray diffraction techniques. Scanning electron microscopy (SEM) investigations were conducted in a JEOL™ Model JSM-T330 operated at 25 kV and linked with a Zmax 30 Boron-up light element energy dispersive spectrometer (EDS) detector. For the SEM investigations, optical mount specimens were prepared using standard metallographic techniques followed by chemical etching in a HF solution (5%) for 1.5 min. The etched optical samples were coated with carbon.

The X-ray diffraction investigations were carried out in a Philips™ Model PW3710 using CuK_α radiation at 40 kV and 40 mV settings in the 2θ range from 10 to 90°. The crystallized phases were identified by comparing the peak positions and intensities with those in the JCPDS (Joint Committee on Powder Diffraction Standards) data files.

3. Results and discussion

Tanaka et al.[9] reported that glass formation in the binary $(1-x)TeO_2 + xLiCl$ system takes place with LiCl contents varying between 0.15 and 0.6 mol. The present study is part of an ongoing investigation on the $(1-x)TeO_2 + xLiCl$ glasses doped with $0.005Tm_2O_3$ (0.5 mol% Tm_2O_3). After a series of preliminary DTA and X-ray diffractometry tests, three compositions, viz. $x = 0.3$, 0.35 and $x = 0.4$ mol, were chosen which yielded a homogeneous glass matrix. The Tm^{3+} ion is doped to exhibit absorption and luminescence transitions in the TeO_2–LiCl glasses intended for solid state laser applications.[8] The thermal and optical properties of Tm^{3+} doped TeO_2–LiCl glasses have been reported elsewhere[26] and is beyond the scope of the present work. However, it should be mentioned here that the addition of 0.005 moles of Tm_2O_3 has no effect on the microstructure and the crystallization behaviour of the TeO_2–LiCl glasses of the present investigation. Further, due to its low content, the presence of Tm_2O_3 can not be verified in either SEM or X-ray diffractometry analyses of the present study.

3.1. Thermal analysis and microstructural characterization

Differential thermal (DTA) investigations were conducted on the as-cast TeO_2–LiCl glasses. Fig. 1 shows the respective DTA data of the as-cast $0.6TeO_2$–0.4LiCl, $0.65TeO_2$–0.35LiCl and $0.7TeO_2$–0.3LiCl glasses scanned at a rate of 10°C/min between 25 and 600°C. As seen in Fig. 1, the DTA scans exhibit small endothermic peaks at 260°C for the $0.6TeO_2$ –0.4LiCl glass, at 265°C for the $0.65TeO_2$–0.35LiCl glass and at 272°C for the $0.7TeO_2$ –0.3LiCl glass selected as the glass transition temperature, T_g. Crystallization processes taking place in the glass matrix are marked by exothermic peaks at 401°C for all glass samples, indicating that the crystallization mechanism for the three samples are the same. As expected, the area under the exothermic peak and its height increase with decreasing LiCl content. The exothermic peaks correspond to the peak crystallization

temperatures, T_p for both materials. The T_g values of the present investigation are higher than those reported by Tanaka et al.[9] for the $(1-x)TeO_2+xLiCl$ due to the fact that they used a smaller heating rate of 2.5 °C/min during their T_g measurements. In addition, as seen in Fig. 1, T_g shifts to lower values and the height/area of the exothermic peak decreases with the increasing LiCl content. As discussed by Tanaka et al.[9] this expected behaviour is attributed to the fact that LiCl acts as a network modifier and breaks down the TeO_4 network structure with creating the non-bridging oxygen in Li_2O. On the other hand, with increasing contents of TeO_2 the formation of TeO_3 trigonal pyramids is enhanced.[9]

On the basis of DTA results, X-ray diffractometry scans were carried out to verify the nature of crystallizing phase(s) in the glassy matrix at temperatures above T_c for both materials. X-ray diffractometry patterns of the as-cast $0.6TeO_2$ –0.4LiCl, $0.65TeO_2$ – 0.35LiCl and $0.7TeO_2$ –0.3LiCl glasses revealed no detectable peaks, indicating the fact that they consist of only amorphous glass matrix in the as-cast state. On the other hand, X-ray diffractometry scans of the as-cast glass samples heated to 425°C (above the peak crystallization temperature) at a rate of 10°C/min followed by quenching in air showed the evidence of devitrification. Fig. 2(a) and (b) show the X-ray diffraction patterns taken from the $0.6TeO_2$–0.4–LiCl and $0.7TeO_2$–0.3LiCl glass samples, respectively. All the peaks in Fig. 2(a) and (b) matched the *d*-values of the paratellurite (TeO_2) phase which has a tetragonal crystal structure with lattice parameters $a=0.481$ nm and $c=0.761$ nm.[27] Only three crystal peaks can be detected for the LiCl-rich sample, i.e. for the $0.6TeO_2$ – 0.4LiCl glass [Fig. 2(a)]. It can be deduced that the paratellurite phase has crystallized in small quantities in a predominantly glass matrix. On the other hand, almost all the reflection planes of the paratellurite phase in the $0.7TeO_2$ –0.3LiCl glass are detected in the XRD scan of Fig. 2(b), an indication of widespread crystallization in the glass matrix. The results of Fig. 2(a) and (b) conform very well with the corresponding shallow and steep crystallization peaks shown in Fig. 1. As expected, the XRD diffractometry pattern of the heat-treated and quenched $0.65TeO_2$ –0.35LiCl glass revealed the presence of only the above-mentioned paratellurite (TeO_2) phase with less crystalline peaks than that for the $0.7TeO_2$ –0.3LiCl glass and more than that for the $0.6TeO_2$ –0.4LiCl glass.

To investigate the morphology of the resultant microstructure after crystallization, SEM investigations were conducted on the TeO_2–LiCl glass samples heated to 425°C followed by air quenching. Fig. 3(a) and (b) are respective SEM micrographs of the $0.6TeO_2$–0.4LiCl sample taken in the secondary electron imaging (SEI) and the back-scattered electron (BEI) imaging modes showing trigonal-shaped crystals between 40 and 50 μm in length and 7 and 15 μm in width. EDS analysis

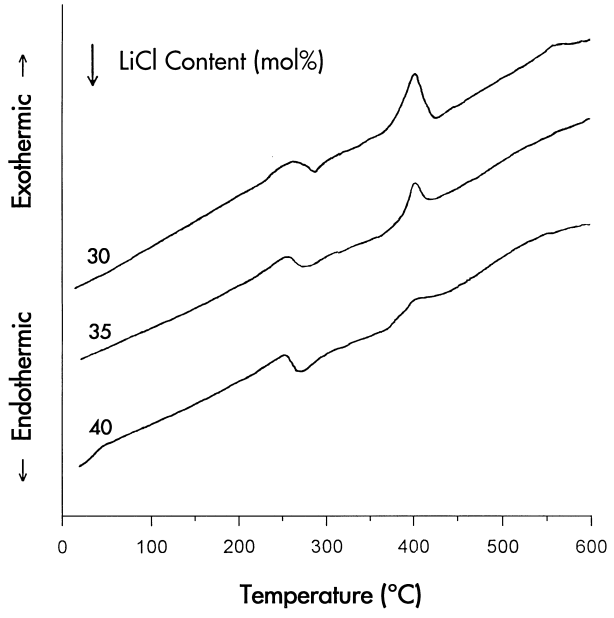

Fig. 1. DTA plots of the $0.6TeO_2$–0.4LiCl, $0.65TeO_2$ –0.35LiCl and $0.7TeO_2$ –0.3LiCl glasses.

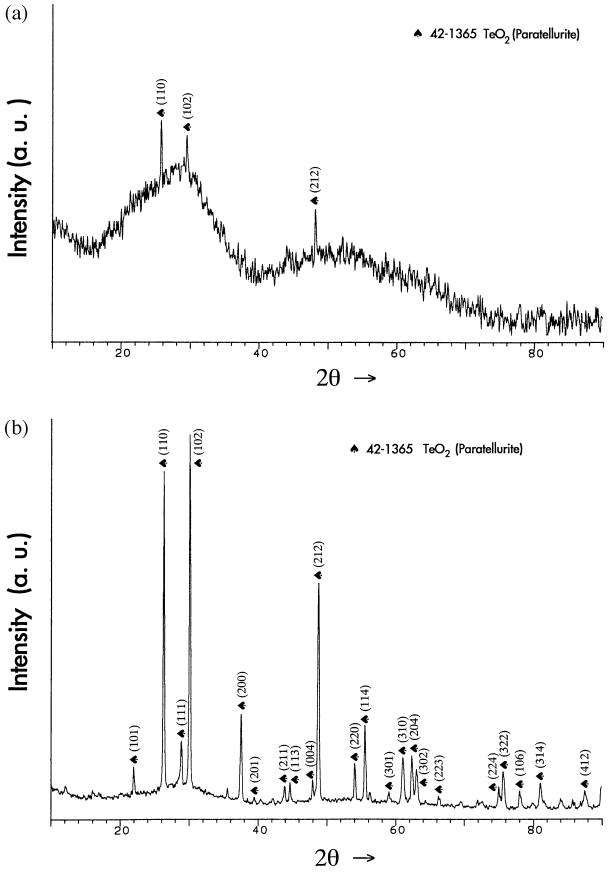

Fig. 2. X-ray diffraction pattern of the (a) $0.6TeO_2$ –0.4LiCl glass and (b) $0.7TeO_2$–3LiCl glass heated at a rate of 10°C/min to 425°C followed by quenching in air.

taken from these crystals [Region T in Fig. 3(a)] revealed that they contained 33.3 at.% Te, 66.6 at.% O and 0.1 at.% Cl. Thus, it is evident that these are paratellurite crystals and they are surrounded by [Region G in Fig. 3(a) the amorphous glassy matrix. In addition, as seen in the SEM-BEI micrograph [Fig. 3(b)], the depth of the paratellurite crystals into the glass matrix is very shallow. Thus, on the basis of Figs. 3(a) and (b), it can be inferred that paratellurite crystals must have formed as a result of surface nucleation. Fig. 4(a) is a SEM/SEI micrograph of the $0.7TeO_2$ –0.3LiCl glass showing the presence of a cluster of large trigonal-shaped crystals varying between 35 and 50 μm in length and 7 and 15 μm in width which were grown centrosymmetrically. The shape of these crystals are almost identical to those for the $0.6TeO_2$ –0.4LiCl [Fig. 3(a)] sample. Fig. 4(b) is a cross-sectional SEM/SEI micrograph taken at a tilt angle of 75° from the same region in Fig. 4(a) which reveals that these crystals [indexed as T and TT in Fig. 4(a)] extend longitudinally on the surface of the sample and the crystal indexed as TT is in the vicinity of the coss-section and has a depth of varying between 5 and 9 μm. The presence of such large crystals having shallow depths with a distinct boundary into the glass matrix indicates the fact that surface crystallization is also predominant in the $0.7TeO_2$–0.3LiCl sample. This is in agreement with the findings of Ray et al.,[28] who revealed that a distinct boundary existing between the glass matrix and the crystallized region during surface crystallization. EDS spectra taken from five different locations on these crystals [Regions T in Figs. 4(a) and T and TT in Fig. 4(b)] have shown that they contained 66.6±0.4 at.% O, 33.2±0.3 at.% Te and 0.1±0.0 Cl. Thus, similar to the $0.6TeO_2$ –0.4LiCl glass, the trigonal-shaped crystals are composed of the paratellurite (TeO_2) phase surrounded by the amorphous glassy matrix [Regions G in Fig. 4(a) and (b)] in the $0.7TeO_2$–0.3LiCl glass, as expected. Overall, the morphology, orientation and size of these crystals clearly indicate that paratellurite crystals formed in both glass systems as a result of surface crystallization. Same trigonal-shaped paratellurite (TeO_2) crystals are also detected in the glass matrix of the $0.65TeO_2$–0.35LiCl material. From these investigations, it can be stated that the

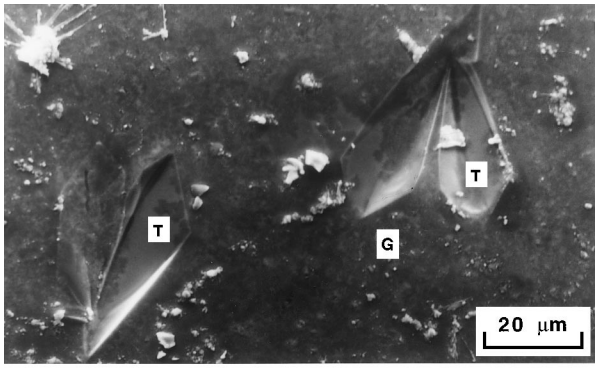

(a)

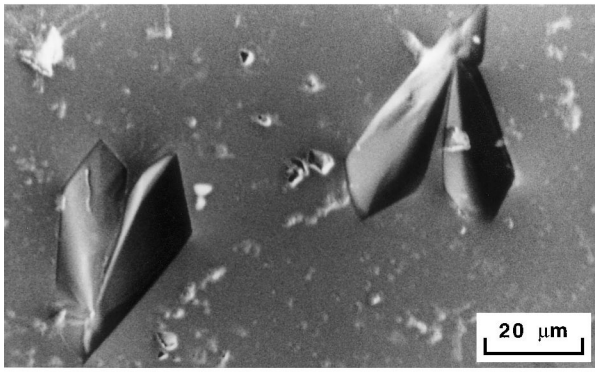

(b)

Fig. 3. Representative (a) SEM/SEI and (b) SEM/BEI micrograph of the $0.6TeO_2$–0.4LiCl glass heated at a rate of 10°C/min to 425°C followed by quenching in air.

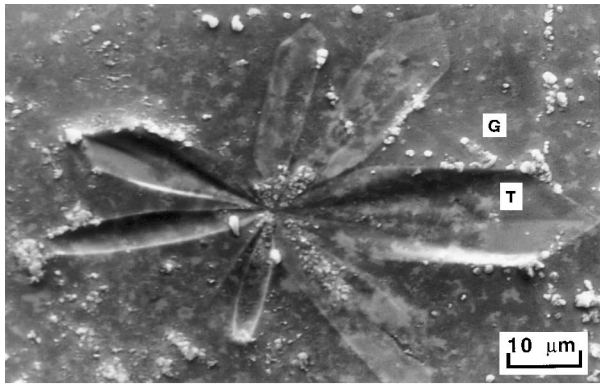

(a)

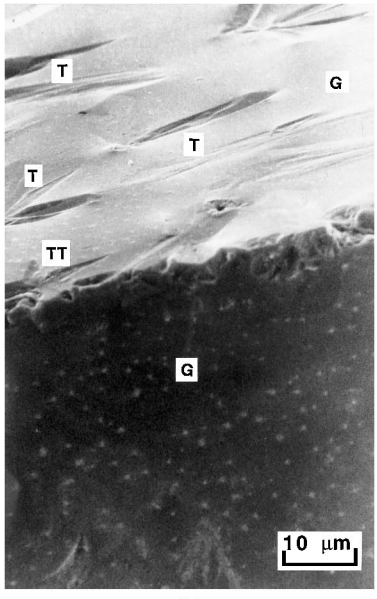

(b)

Fig. 4. Representative (a) SEM/SEI and (b) cross sectional SEM/SEI micrograph of the $0.7TeO_2$–0.3LiCl glass heated at a rate of 10°C/min to 425°C followed by quenching in air.

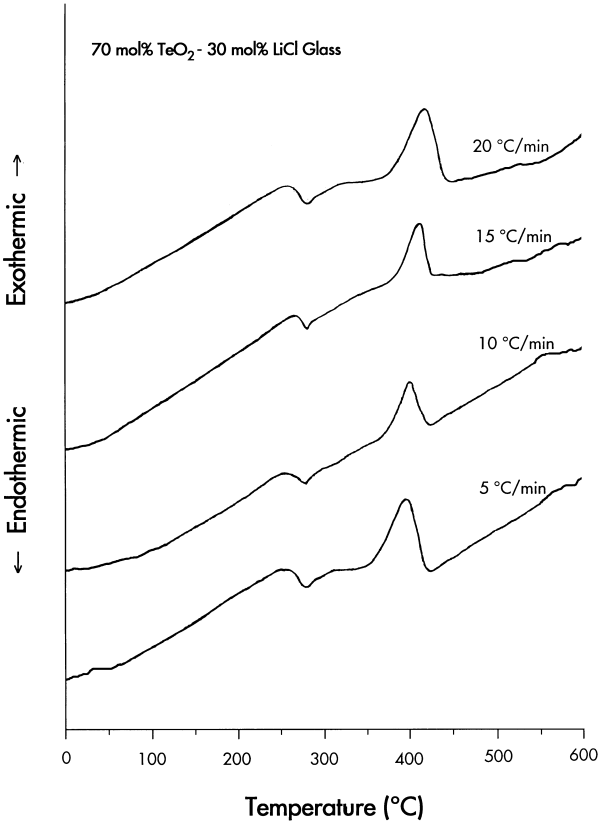

Fig. 5. DTA curves of the $0.7TeO_2$–0.3LiCl glasses scanned at heating rates of 5, 10, 15 and 25°C/min.

paratellurite TeO_2 phase is the only crystallizing phase for the $x TeO_2$–$(1-x)$LiCl glasses in the composition range between $x = 0.6$–0.7 mol.

In the following section, the graphical determination of the activation energy for surface crystallization of the paratellurite phase in the $0.7TeO_2$–0.3LiCl system is presented.

3.2. Activation energy determination

Fig. 5 shows the DTA thermogram of the as-cast $0.7TeO_2$ –0.3LiCl glass sample scanned at the heating rates of 5, 10, 15 and 20°C/min. The T_g and T_p values for different heating rates are listed in Table 1. As expected, both the T_g and T_p temperatures shift to higher values with increasing rate, a behaviour also reported in the DTA studies of other glass systems.[29–33]

The shift of peak temperatures with heating rate in a nonisothermal DTA study was first analyzed by Kissinger[29,30] in the study of kinetics of chemical reactions. DTA is suitable for studying the crystallization of glass[31–33] and the DTA curves shown in Fig. 5 can be used to determine the activation energy for crystal growth by analyzing the peak crystallization temperatures.[34] As shown by Matusita and Sakka,[35] if the number of crystal nuclei formed at temperatures above T_g can be assumed constant in a glass matrix, then the

Table 1
Heating rate, glass transition and peak crystallization temperatures of the $0.7TeO_2$-0.3LiCl sample detected during the DTA scans[a]

B (°C/min)	T_g (°C)	T_p (°C)
5	269	394
10	272	401
15	276	408
20	279	415

[a] The T_g values are measured at the mid-point between the onset and the minimum temperatures of the glass transition endotherm and the T_p are measured at the peak of the crystallization exotherm during the DTA scans.

rate of change of volume fraction of crystals can be defined as:

$$\frac{dx}{dt} = KB^{-(n-1)}(1-x)^k \exp\left(-\frac{mQ}{RT}\right) \quad (1)$$

with its maximum at $T = T_p$ for any non-isothermal DTA condition. Therefore, as stated by Matusita and Sakka,[35] Eq. (1) can be solved at $\left(d^2x/dt^2\right) = 0$ and re-expressed as:

$$\ln\left(\frac{B^n}{T_p^2}\right) = -\frac{mQ}{RT_p} + \text{constant} \quad (2)$$

assuming that the term $(1-x_c)^k$ is constant for $x = x_c$, $T = T_p$. Thus it seems that the three unknowns in Eq. (2) can be calculated using the parameters B and T_p given in Table 1 in four equations. As stated previously, the paratellurite (TeO_2) crystals form as a result of surface crystallization. Thus, $n = m = 1$ for all heating rates can be assumed which leads to the Kissinger equation:[29]

$$\ln\left(\frac{B}{T_p^2}\right) = -\frac{Q}{RT_p} + \text{constant} \quad (3)$$

Fig. 6 is a graphical solution of the Eq. (3) where the T_p and B values listed in Table 1 are used to plot $\ln(B/T_p^2)$ as a function of $1/T_p$ to calculate the activation energy for crystallization. As seen in Fig. 6, parameters measured in four different non-isothermal DTA analyses provide a linear fit of data points and the slope is nothing but Q/R (where $R = 8.31$ J/K-mol, gas constant). The activation energy, Q can then be calculated as 238 kJ/mol. Since paratellurite crystallization in TeO_2-based glasses and glass-ceramics have been not reported in the literature, this value can only be compared to the activation energies of crystal growth in SiO_2-based glasses and glass-ceramics. This value is larger than the activation energy value of 150 kJ/mol for surface crystallization of the diopside phase in a SiO_2-rich glass-ceramic nucleated

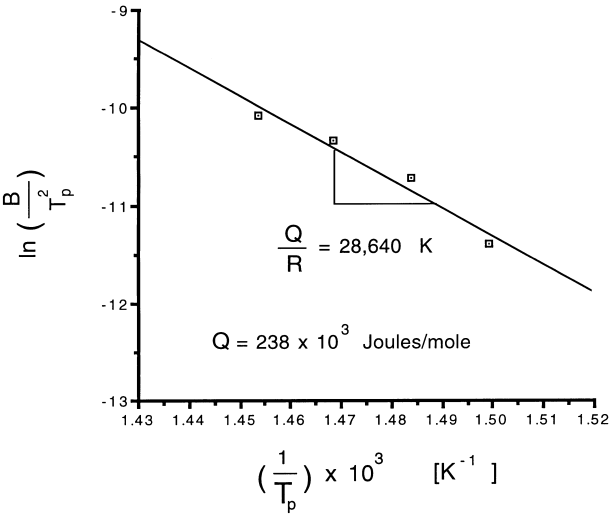

Fig. 6. Graphical determination of the activation energy for surface crystallization of the paratellurite phase in the $0.7TeO_2$–$0.3LiCl$ glass; Kissinger plot of data obtained from DTA curves in Fig. 5 and reported in Table 1.

with TiO_2 in the quaternary SiO_2–MgO–Al_2O_3–CaO system[34] it is comparable to the activation energy values of 256±11 kJ/mol for the $MgTi_2O_5$ phase and 275±6 kJ/mol for the mica phase crystallization in a SiO_2-based multicomponent glass.[36]

4. Conclusions

On the basis of the results reported in the present investigation, the following conclusions can be drawn:

1. Devitrification of the $(1-x)TeO_2$–$xLiCl$ (with $x=0.3$–0.4 mol) glasses doped with 0.005 mol of Tm_2O_3 takes place in the vicinity of 400°C with the formation of the paratellurite (TeO_2) as the only crystallizing phase in the glassy matrix.
2. The paratellurite crystals form in the $(1-x)TeO_2$–$xLiCl$ (with $x=0.3$–0.4 mol) glasses as a result of surface nucleation, they are trigonal in shape and have a size range between 40 and 50 μm in length, 7 and 15 μm in width and they penetrate into the glass matrix at depths varying between 4 and 9 μm.
3. Using the analysis of Matusita and Sakka, the activation energy for surface crystallization in the $0.7TeO_2$ –$0.3LiCl$ glass was calculated as 238 kJ/mole from the slope of the Kissinger plot.

Acknowledgements

The authors would like to express their gratitude to Prof. Dr. D. Ülkü for serving as technical advisor for the TTGV-180/S (Technology Development Foundation of Turkey) project out of which this investigation has emerged. We also acknowledge the help and contribution of Ms. Nurten Dinçer during the SEM and DTA investigations of this study. This research has been partially supported by the Research Foundation of Istanbul Technical University under the contract number 594.

References

1. El-Shafi, N. A. and Morsi, M. M., Optical absorption and infrared studies of some silicate glasses containing titanium. *J. Mater. Sci.*, 1996, **32**, 5185–5189.
2. Nageno, Y., Takebe, H., Morinaga, K. and Izumitani, Effect of modifier ions on fluorescence absorption of Eu^{3+} in alkali and alkali earth silicate glasses. *J. Non-Cryst. Solids*, 1994, **169**, 288–294.
3. Nageno, Y., Takebe, H. and Morinaga, K., Correlation between radiative transition probabilities of Nd^{3+} and composition in silicate, borate and phosphate glasses. *J. Am. Ceram. Soc.*, 1993, **76**(12), 3081–3086.
4. Stanworth, J. E., Tellurite glasses. *Nature*, 1952, **169**, 581–582.
5. Wang, J. S., Vogel, E. M. and Snitzer, E., Tellurite glasses: a new candidate for fiber devices. *Opt. Mater.*, 1994, **3**, 187–203.
6. Kim, S. H. and Yoko, T., Nonlinear optical properties of TeO_2-based glasses: MO_x–TeO_2 (M = Sc, Ti, V, Nb, Mo, Ta and W) binary glasses. *J. Am. Ceram. Soc.*, 1995, **78**(4), 1061–1065.
7. Burger, H., Vogel, W. and Kozhukharov, V., IR transmission and properties of glasses in the tellurium oxide (TeO_2)-[R_nO_m, R_nX_m, $R_n(SO_4)_m$, $R_n(PO_3)_m$ and boron oxide] systems. *Infrared Phys*, 1995, **25**, 395–401.
8. Özen, G., Denis, J-P., Genotelle, M. and Pellé, F., T_m-Y_b-T_m energy transfers effect of temperature on the fluorescence intensities in oxyfluoride-telluride compounds. *J. Phys.: Condens. Matter*, 1995, **7**, 4325–4336.
9. Tanaka, K., Yoko, T., Yamada, H. and Kamiya, K., Structure and ionic conductivity of LiCl–Li_2O–TeO_2 glasses. *J. Non-Cryst. Solids*, 1994, **169**, 288–294.
10. Sahar, M. R., Jehbu, A. K. and Karim, M. M., TeO_2–ZnO–$ZnCl_2$ glasses for IR transmission. *J. Non-Cryst. Solids.*, 1997, **213&214**, 164–167.
11. Kosuge, T., Benino, Y., Dimitrov, V., Sato, R. and Komatsu, T., Thermal stability and heat capacity changes at the glass transition in K_2O–WO_3–TeO_2 glasses. *J. Non-Cryst. Solids*, 1998, **242**, 154–164.
12. Komatsu, T., Naguchi, T. and Benino, Y., Heat capacity changes and structural relaxation at glass transition in mixed-alkali tellurite glasses. *J. Non-Cryst. Solids*, 1997, **222**, 206–211.
13. Kim, H. G., Komatsu, T., Shioya, K., Matusita, K., Tanaka, K. and Hirao, K., Transparent tellurite-based glass-ceramics with second harmonic generation. *J. Non-Cryst. Solids*, 1998, **208**, 303–307.
14. Safonov, V. V., Ovcharenko, N. V., Bayandin, D. V. and Krylov, I. A., Interactions and the properties of glasses in the PbO–TeO_2–WO_3 system. *J. Inorganic Chem.*, 1992, **37**(7), 833–835.
15. Singh, R., Glass transition temperature and the structure of TeO_2–V_2O_5–Fe_2O_3 glasses. *J. Phys. D: Appl. Phys*, 1987, **20**, 548–551.
16. Ford, N. and Holland, D., Optical and physical properties of glasses in the systems GeO_2–Bi_2O_3–PbO and TeO_2–Bi_2O_3–WO_2. *Glass Tech.*, 1987, **28**(2), 106–113.
17. Kim, H. Y., Komatsu, T., Sato, R. and Matusita, K., Incorporation of $LiNbO_3$ crystals into tellurite glasses. *J. Mater. Sci.*, 1996, **31**, 2159–2164.
18. Yakhkind, A. K., Tellurite glasses. *J. Am. Ceram. Soc.*, 1966, **49**(12), 670–675.

19. Brady, G. W., X-ray study of tellurium oxide glasses. *J. Chem. Phys*, 1956, **24**, 477–481.
20. Brady, G. W., Structure of tellurium oxide glasses. *J. Chem. Phys*, 1957, **27**, 300–303.
21. Shimzugawa, Y., Maeseto, T., Suehara, S., Inoue, S. and Nukui, A., EXAFS and RDF studies of TeO_2–Li_2O glasses. *J. Mater. Res*., 1995, **10**, 405–410.
22. Nishida, T., Yamada, M., Ide, H. and Tkashima, Y., Correlation between the structure and glass transition temperature of potassium, magnesium and barium tellurite glasses. *J. Mater. Sci*., 1990, **25**, 3546–3550.
23. Sakida, S., Hyakawa, S. and Yoko, T., ^{125}Te NMR study of M_2O–TeO_2 (M = Li, Na, K, Rb, Cs) glasses. *J. Non-Cryst. Solids*, 1999, **243**, 13–25.
24. Reau, R., Tanguy, B., Portier, J., Rojo, J. M., Sanz, J. and Herrero, M. P., Influence of the fluorine-oxygen substitution on the ionic conductivity properties of lithium tellurite glasses. *J. de Physique (Colloque C2)*, 1992, **2**, 165–170.
25. Bahgat, A. A., Shaltout, I. I. and Abu-Elazm, A. M., Structural thermal properties of some tellurite glasses — section 4. Spectroscopy. *J. Non-Cryst. Solids*, 1992, **150**, 179–184.
26. Özen, G., Demirata. & Öveçoğlu, M.L., Thermal and optical properties of Tm^{3+} doped tellurite glasses. *Spectrochimica Acta*, 2000, in press.
27. *Powder Diffraction File*, Card no. 42-1365 *1992 Database Edition,* Joint Committee on Powder Diffraction Standards, Swathmore, PA, USA.
28. Ray, C. S., Yang, Q., Huang, W-H. and Day, D. E., Surface and internal crystallization in glasses as determined by differential thermal analyses. *J. Am. Soc*., 1996, **79**(12), 3155–3160.
29. Kissinger, H. E., Variation of peak temperature with heating rate in differential thermal analysis. *J. Res. Nat. Bur. Stand*, 1956, **57**, 217–221.
30. Kissinger, H. E., Reaction kinetics in differential thermal analysis. *Anal. Chem*., 1957, **29**, 1702–1706.
31. Thakur, R. L. and Thiagarajan, S., Studies in catalyzed crystallization of glasses: a DTA method. *Cent. Glass Ceram. Res. Inst. Bull*, 1966, **13**, 33–45.
32. Skvára, F. and Satava, V., Kinetic data from DTA measurements. *J. Thermal Anal*, 1970, **2**, 325–335.
33. Sestak, J., The applicability of DTA to the study of crystallization kinetics of glasses. *Physics and Chemistry of Glasses*, 1974, **15**(6), 137–140.
34. Öveçoglu, M. L., Kuban, B. and Özer, H., Characterization crystallization kinetics of a diopside-based glass-ceramic developed from glass industry raw materials. *Journal of the European Ceramic Society*, 1997, **17**, 957–962.
35. Matusita, K. and Sakka, S., Kinetic study on crystallization of glass by differential thermal analysis — criterion on application of Kissinger plot. *J. Non-cryst. Solids*., 1980, **38&39**, 741–746.
36. Cheng, K., Wan, J. and Liang, K., Differential thermal analysis on the crystallization kinetics of K_2O–B_2O_3–MgO–Al_2O_2–SiO_2–TiO_2–F glass. *J. Am. Ceram. Soc*., 1999, **82**(5), 1211–1216.